The Role of Heat and Momentum Exchange at the Sea Surface in Radiative-Convective Equilibrium

Master thesis of
Wouter Mol
Utrecht University, IMAU

Supervised by:
dr. Aarnout van Delden (Utrecht University)
dr. ir. Chiel van Heerwaarden (Wageningen University & Research)

January 14, 2019

Abstract

Radiative-convective equilibrium (RCE) is an idealized representation of the tropical atmosphere in which net radiative cooling fluxes are compensated by convective heat fluxes. In large domain RCE experiments with cloud resolving models, or coarser models, convection can show large scale spontaneous organisation referred to as 'convective self-aggregation'. This type of convective organisation happens despite uniform initial and boundary conditions and an absence of large scale forcing. This phenomenon is important to understand, because it has a significant impact on the domain-mean climate. It is not very well understood yet, partly due to generally poor agreement among model studies. A contributor to this poor agreement is the sensitivity of convective self-aggregation to almost any model parameter. In an attempt to further investigate this phenomenon, a model intercomparison project, RCEMIP, has been set up; each participating modelling group performs the same experiment with their own model. Coarse models are not expected to accurately resolved near-surface turbulence. One way of parametrizing the resulting underestimation of surface fluxes and prevent numerical issues in the free convection limit, is by enforcing a minimum value for the wind speed that is put into the surface layer formulation scheme. In the proposed simulations of RCEMIP, a value of $\mathrm{U_{min}}$ = 1 m s^{-1} is used for models that apply this solution. Limited domain large eddy simulations (LES) are performed using MicroHH to see what the effect of $\mathrm{U_{min}}$ = 1 m s^{-1} is on the evolution of the RCE state, compared to a value closer to zero. We find that the majority of the domain in these experiments have winds below 1 m s^{-1} at any time during the 20 to 30 days of simulation. Averaged over regions where the lowest-level wind speed is below 1 m s^{-1}, latent heat fluxes are increased by as much as 20%. This would mean that enforcing a minimum wind speed of 1 m s^{-1} reduces the flux contrast between the calm environment and convective regions, thereby reducing the strength of the surface flux feedback as a self-aggregation mechanism. The spatial variance in the near-surface moisture field increases with a higher value for $\mathrm{U_{min}}$, however. Performing the same kind of experiment, but with a set-up that would allow self-aggregation to occur, is suggested to further understand the impact of changes to the surface flux feedback mechanism.

1 Introduction

Radiative-convective equilibrium (RCE) is an idealized representation of the tropical atmosphere in which cooling due to net outgoing radiation is compensated by heating through convection. In recent years, RCE modelling is being used to study the phenomenon of self-aggregation of tropical deep moist convection, first observed by Held, Hemler, and Ramaswamy (1993). Though there are many different modes of convective organisation, self-aggregation refers to an organisation on the scale hundreds of kilometres. More specifically, it is a mode of organisation that appears to form spontaneously in certain RCE model experiments, despite homogeneous initial and boundary conditions and no large scale forcing. This phenomenon is not observed in all simulations and is sensitive to both the numerical and physical configuration of the model. Understanding the mechanisms and impact of self-aggregation has proven to be challenging. Contradictions and debate in literature are indicative for the still incomplete understanding of the physics involved and poor ability to accurately simulate an atmosphere in RCE, although progress has been made in recent years. A thorough discus-

sion of this topic is presented in the review paper on convective self-aggregation by Wing, Emanuel, Holloway, and Muller (2017).

Large scale self-aggregation of convection is an important phenomenon to understand, given that the domain-mean climate of these aggregated states differs from that of non-aggregated, more scattered convection. Significant drying in the aggregated state is one of the more notable differences, in particular in the free troposphere where the relative humidity (RH) gets as low as 20%. The free troposphere is consequently also a few degrees warmer and outgoing long-wave radiation is more efficient, increasing by 10-30 W m^{-2} (Wing et al., 2017). However, the magnitudes of these effects are reduced when the degree of aggregation is lower.

One of the points of discussion is the effect of sea surface temperature (SST) on the occurrence and, if present, the magnitude of the aggregated state. It could lead to a negative feedback to the global warming since more heat is lost to space in aggregated states. Before the question can be answered, a more robust understanding of the physics involved and ability to accurately simulate RCE must be achieved. A significant effort is being made currently by the organisation of a Radiative-Convective Equilibrium Model Intercomparison Project (RCEMIP, Wing, Reed, Satoh, Stevens, Bony, and Ohno (2018)).

One mechanism favouring self-aggregation is the surface flux feedback, though in the rotation-free case it is not in itself enough to cause self-aggregation (Wing et al., 2017). The extra contribution of increased wind speed in convective regions to the latent heat flux is stronger than the decrease in the atmosphere-ocean specific humidity imbalance. The idea is thus that moister, convective regions experience enhanced fluxes compared to drier, calm regions, (further) increasing the contrast between the two.

The exchange of sensible heat, moisture, momentum are not calculated explicitly, but through a parametrization scheme, also referred to as a surface layer formulation. This formulation couples the atmospheric surface layer (ASL) to the model bottom boundary, here taken to be a sea surface. A problem arises as a consequence of this approach when simulating with free convection, i.e. an unstable boundary layer and no wind. One way of dealing with this problem is applying a minimum value for the wind speed, $\mathrm{U_{min}}$, used in the parametrization. The theory of this topic will be further discussed in section 2.

The aim of this research is to find out to what extent RCE simulations, following the RCEMIP case description, are sensitive to the chosen value for $\mathrm{U_{min}}$ = 1 m s^{-1} as is suggested in Wing et al. (2018). Performing large eddy simulation (LES) on small domains will allow the explicit resolving of near-surface turbulence in the free convection regime and a value for $\mathrm{U_{min}}$ closer to zero. Though the small domain size prevents self-aggregation from occurring, a look is taken into how the surface flux feedback mechanism would be affected. Theoretically, larger values of $\mathrm{U_{min}}$ could lead to an underestimation of the feedback strength, as latent heat fluxes are increased in calm regions, thus reducing the contrast between calm and convective regions. The focus is on latent heat fluxes, as those are a factor 10 larger than sensible heat fluxes in a typical tropical climate. The method, including the case and model description, is discussed in section 3. The results and discussion are presented in sections 4 and 5 followed by the conclusions in 6.

2 Theory

2.1 The surface layer formulation and dealing with free convection

Since the exchange of sensible heat, moisture and momentum between a surface and the air directly above it cannot be explicitly solved, a parametrization is required. What is nearly always used in numerical models of the atmosphere, are parametrization schemes based on Monin-Obukhov Similarity Theory (MOST) (chapter 10 of Wyngaard (2010)). This similarity theory related surface fluxes of sensible heat, moisture and momentum to their respective near-surface gradients using functions fitted to observational data. These functions depend on $\zeta = z_1/L$, where z_1 is the height of the lowest model level and L the Obukhov length defined as follows:

$$L \equiv -\frac{u_*^3}{\kappa B_0} \tag{2.1}$$

u_* is the surface friction velocity, $\kappa = 0.4$ the Von Karman constant and B_0 the surface kinematic buoyancy flux. The empirical functions, ϕ_m and ϕ_h, are different in unstable ($\zeta < 0$) and stable ($\zeta > 0$) conditions. Since we are discussing surface fluxes in a RCE set-up, conditions are nearly always unstable and so only the functions for the unstable case will be further discussed. The physical interpretation of $-L$ in unstable conditions is the height at which turbulent kinetic energy (TKE) generation due to buoyancy becomes equal to that the generation of TKE due to wind shear. Below $-L$, TKE generation due to shear is more important. equation 2.1 directly relates u_* to L, so increased near-surface wind speeds also increase u_*. The general

form of the empirical functions is:

$$\phi_{m,h} = (1 + \gamma_{m,h}|\zeta|^{\alpha_1})^{\alpha_2} \tag{2.2}$$

Throughout the years, many different attempts have been made at finding the best values of the coefficients for fitting equation 2.2 to observational data. The fit can be optimized for different regimes of ζ, but also depends on the quality of the observational data. For example, Högström (1988) presents updated values of $\gamma_{m,h}$ for various choices of α_1 and α_2 based on improved observational data. More recently, Wilson (2001) found that setting $\alpha_1 = 2/3$ and $\alpha_2 = -1/2$ has the correct asymptotic behaviour in the free convection limit while also fitting well to more weakly unstable conditions. Additionally, it made integrating the functions more simple. Both of these reasons are why the proposed equations by Wilson (2001) are adopted in the model (section 3.1) we use for this research.

What if there is no wind, as is the case in the free convection limit? L will become zero, explained physically by the fact that TKE production due to wind shear will not be higher anywhere in the surface layer as there is no wind shear. This gives

$$\lim_{L \to 0-} \zeta = z_1/L = -\infty \tag{2.3}$$

and poses a problem for finding the surface flux. There are multiple ways of dealing with this, the simplest of which is applying a minimum value to the wind speed U_1 at height z_1 in the surface flux calculation as such:

$$U_1 = \max(U_1, \mathrm{U_{min}}) \tag{2.4}$$

A more advanced method is used by the ECMWF in their IFS model (see their section 3.2.1 of ECMWF (2018)) based on the work of Beljaars (1995). An extra term is added to the calculation of U_1:

$$|U_1|^2 = u_1^2 + v_1^2 + w_*^2 \tag{2.5}$$

where u and v are the horizontal components of the wind speed and w_* is the so called free convection velocity scale. This extra term represents wind induced by large eddies in the free convection regime, based on LES data, ensuring L cannot reach 0. This method cannot be used in LES however, as the turbulence is calculated explicitly and adding such an extra term would in essence count the turbulent velocity twice. Mind that for both methods of dealing with L becoming zero, the diagnostic variables u and v are not directly affected, but only the derived value of U_1 that gets passed into the parametrization.

2.2 Cold pools and the environment

Cold pools are regions with relatively low temperatures in the lowest few hundred meters of the atmosphere. They are caused by rain evaporation in downdrafts of convective cells, and, if the precipitation rate is high enough, also by bringing down air with lower θ_e from aloft (Zuidema, Torri, Muller, and Chandra, 2017). The formation of stronger cold pools characterized by low θ_e values can also be seen as density currents. Once the downdraft with low θ_e air from aloft reaches the surface, there is no way to go but spread out horizontally, creating gust fronts along the leading edge of the higher density air. Newly formed cold pools and gust fronts form a contrast with the environment. The environment is defined here as the calm region that is typically free of deep convection, where consequently also the lowest values of U_1 are found.

Schlemmer and Hohenegger (2015) found that moisture advection is, by far, the main contributor to the temporal evolution of the near-surface moisture budget. Both for cold pools regions and the environment. Therefore, a qualitative look is taken at these cold pools in the context of this research, despite not being the main focus.

3 Method

3.1 About the model

The numerical model used for the simulations is MicroHH, described in detail in van Heerwaarden, van Stratum, Heus, Gibbs, Fedorovich, and Mellado (2017). One of its capabilities is that of LES of turbulent flows under the anelastic approximation, which is used here. Prognostic variables of the dynamical core include the three velocity components u, v and w, specific humidity q and liquid water potential temperature θ_l. Pressure is solved diagnostically using the Poisson equation. A two-moment warm microphysics scheme is used (based on Seifert and Beheng (2005)), which introduces two more prognostic variables, the rain drop number density n_r and liquid rain water specific humidity q_r. MicroHH uses a staggered C-grid.

Time integration is done with a fourth-order Runge-Kutta scheme using an adaptive time step. Scalars are advected with a second-order scheme that applies third-order interpolation, acting as hyper-diffusion (Wicker and Skamarock, 2002). The scheme will be referred to as `2i3` here. It has the properties of being (near) monotone, smoothing out 4th and higher order structures. This has the advantage of minimizing non-physical tendencies near sharp boundaries, which is for example relevant for the moisture gradient at the top of an

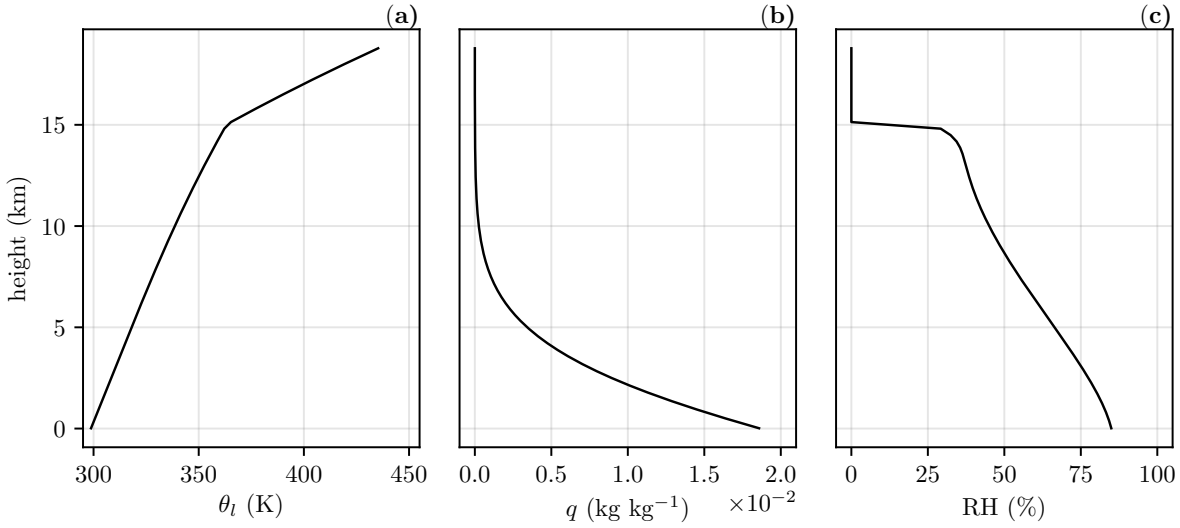

Figure 1 – Initial profiles of the prognostic variables **(a)** θ_l and **(b)** q as a function of height. Approximated relative humidity is shown in **(c)**.

atmospheric boundary layer. A 4th order interpolation variant, `2i4`, is used in a sensitivity experiment to make sure results are not exclusive to numerical schemes with properties similar to that of `2i3`. Subgrid-scale turbulent mixing is handled by a second order Smagorinsky scheme.

As discussed in section 2.1, surface fluxes are calculated using a MOST-based parametrization adapted for the free convection limit, following (Wilson, 2001). For numerical stability, a minimum value for the wind velocity difference between the lowest model level and the surface is set to 0.1 m s^{-1} when passed into the surface layer scheme. There is no (interactive) surface model, meaning the ocean is represented by a constant bottom boundary condition of temperature and specific humidity, so it has an infinite supply of (latent) heat. A sponge layer is applied at above the troposphere in order to prevent gravity waves from reflecting back into the domain.

MicroHH does not yet feature an interactive radiation scheme for solving radiative transfer and resulting temperature tendencies. However, tendencies can be prescribed to prognostic variables such as θ_l, which is used instead of radiation and is further discussed in section 3.2.1.

3.2 Case description

The physical set-up of the simulation will follow, as closely as possible, the case description given by RCEMIP for a SST of 300 K. The initial profiles of θ_l and q are illustrated in figure 1. The bottom boundary condition is a fully saturated surface at 300 K and kept constant throughout the simulation. The model is initialized with $u, v, w = 0$ at every model level. Throughout the simulation, the Coriolis parameter f is set to 0 s^{-1} and any form of large scale forcing is absent. Also absent is a daily cycle, i.e., the applied radiation (more in section 3.2.1) is constant in time, just like all other boundary conditions. Random noise is applied to the θ_l field in the lowest model levels with a maximum amplitude of 0.1 K in order to break the symmetrical initial conditions.

3.2.1 Radiation substitute

Since MicroHH does not yet support interactive radiation, a substitute cooling profile is applied to the prognostic variable θ_l each time integration step. This profile, $\partial\theta_l(z)/\partial t$, is based on the mean net radiative cooling rate of day 70 till 100 in a preliminary System for Atmospheric Modelling simulation of the 300 K RCEMIP case (courtesy of Allison Wing). See figure 2 for an illustration of the profile. In essence, the simulations in this research represent the convective adjustment to the applied large scale atmospheric cooling.

3.3 Simulation overview

A baseline, or reference, simulation is performed on a domain of size 153.6^2 by 19.1 km where the minimum wind speed input for the surface layer formulation, hereafter denoted as $\mathrm{U}_{\mathrm{min}}$, is set to 0.1 m s^{-1}. This simulation is labelled `ldr_reference` and is run for 20 days. The size of the domain is thought be large enough to not be limiting the typical scale of convective cells. These cells are ex-

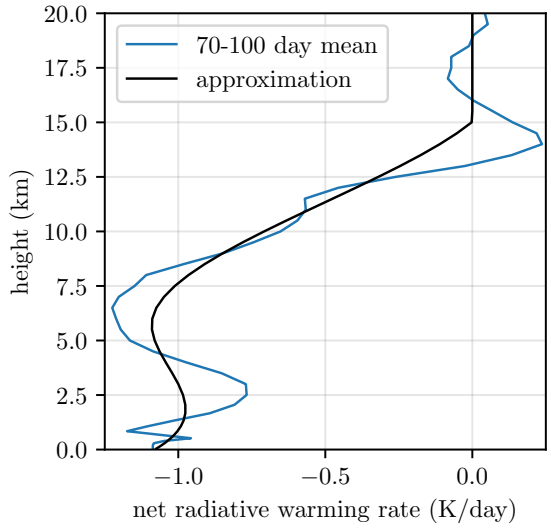

Figure 2 – The temperature tendency due to net outgoing radiation averaged over day 70 to 100 of the SAM RCEMIP simulation (blue) and the approximation used in this research (black), as a function of height.

pected[1] to be short-lived (hours) scattered single or multi cells, typical for a shear-free environment. A resolution of 100 m is used for the horizontal axes and a stretched grid for the vertical axis. The stretching is done to provide a high resolution in the (lower) troposphere where it is most needed, starting at Δz = 30 m at the lowest level, while keeping the amount of vertical levels to a minimum. The resolution is increased by 2% every level, resulting in $\Delta z \approx 350$ m at 19 km. Although the lowest level z_1 of the u and v variables is at a height of 15 m instead of 37 m, as is the case for the RCEMIP experiments, the surface layer is only about 20 meters deep with the strongest gradient closest to the surface. In other words, setting the minimum value for 15 or 37 meters is nearly the same, thanks to the logarithmic nature of the surface layer.

A set-up similar to `ldr_reference` is run, but with U_{min} = 1 m s^{-1}, called `ldr_forced`. Due to the computationally demanding nature of running LES on such a large domain, `ldr_forced` is initialized not at t=0, but using the prognostic fields of `ldr_reference` at t = 14 days.

An additional set of runs are performed on a smaller domain, at 38.4[2] by 18.7 km. This set features a reference and forced simulation identical to the large domain version, though both starting at t = 0 s and run for 30 days. This provides a more lengthy comparison between reference and forced simulations. It also allows for a comparison with the large domain statistics to see if indeed the domain size plays a role in the results, which could help generalizing the result to a larger domain. These two simulations are called `sdr_reference` and `sdr_forced`. See table 1 for an overview.

[1] Based on experience from test experiments

3.3.1 Simulation length

The time scale of self-aggregation in RCE experiments to reach a relatively stable state varies from 15 to 100 days (Wing et al., 2017). Since the surface flux feedback is one of the mechanisms important for the early stages of self-aggregation, and not necessarily the maintenance of the aggregated state, there is no need to run the simulations for this research for periods as long as 100 days. Instead, also motivated by the limiting computational time available, `ldr_reference` is run for 20 days. The set on a small domain is extended to 30 days. Results found are therefore thought to be meaningful for the early stages of simulations that do allow self-aggregation to form.

3.3.2 Sensitivity runs

To improve the confidence in the results, three more sets with varying values of the numerical and physical parameters are run. Each set contains a `ldr_reference` and `ldr_forced` run. All of these are run on the small domain and denoted by `sr`. Each set again features a reference and forced version, every simulation of these three sets is performed with Δx = 200 m. In addition to the coarser resolution, one set uses the `2i4` advection scheme while in another set the radiative cooling is doubled. An overview of all the simulations used in this research is given in table 1.

4 Results

Results based on the performed simulations are presented and briefly discussed in this section. It starts with an overview of the temporal evolution and spatial distribution of the wind and surface fluxes. After the direct and indirect effects of a higher value of $U_{min}$are shown, the section will conclude with results of the sensitivity simulations.

4.1 Temporal differences

For the nearly full length of the small domain forced simulation, i.e. the one with U_{min} = 1 m s^{-1}, the surface latent heat flux (figure 3) remains higher. There is a widespread release of convective potential energy once the first cold pools form by forcing conditionally unstable air past the level of free convection (LFC). `ldr_reference` shows the effect

Table 1 – An overview of all the simulations. All simulations are performed using the SST=300 K case setup. The horizontal resolution of the additional sensitivity runs is halved, but the vertical resolution remains unchanged at Δz = 30 m for the lowest level.

simulation group/name	$\mathbf{U_{min}}$ **(m s^{-1})**	**length (days)**	**notes**
large domain runs			153.6^{2}x19.1 km, Δx = 100 m
`ldr_reference`	0.1	20	-
`ldr_forced`	1	20 (init at 14)	-
small domain runs			38.4^{2}x18.7 km, Δx = 100 m
`sdr_reference`	0.1	30	-
`sdr_forced`	1	30	-
sensitivity runs			38.4^{2}x18.7 km, Δx = 200 m
`sr_reference`	0.1	20	-
`sr_forced`	1	20	-
`sr_2i4_reference`	0.1	20	`2i4` advection scheme
`sr_2i4_forced`	1	20	`2i4` advection scheme
`sr_2xrad_reference`	0.1	20	radiative cooling doubled
`sr_2xrad_forced`	1	20	radiative cooling doubled

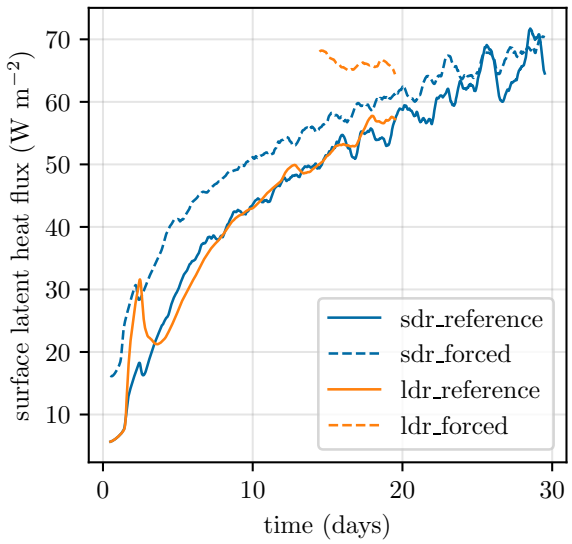

Figure 3 – Time evolution of the surface latent heat flux. A 24-hour centred moving average is applied to better see the difference between simulations.

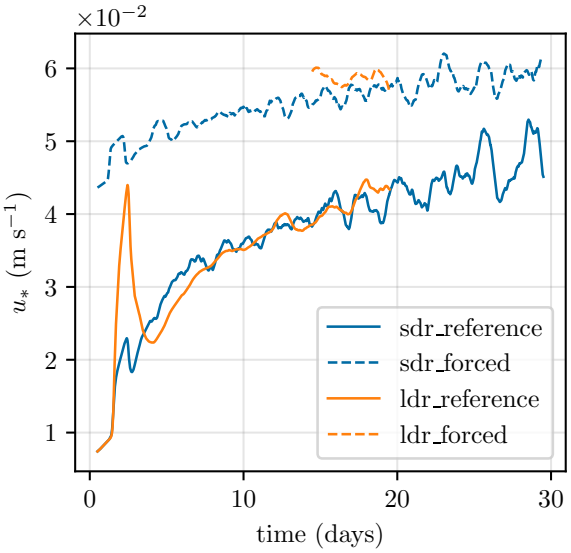

Figure 4 – Time evolution of the surface friction velocity, u_*. A 24-hour centred moving average applied to better see the difference between simulations.

of this release of energy most distinctly by a local peak in both the surface latent heat flux and u_* time series (figure 3 and 4). This phase of the simulation is more an artefact of the uniform nature of the initial conditions of the simulation. Once this first burst of convection has settled down, the physical properties of the boundary layer are more variable in both the horizontal and vertical direction. Towards the end of the simulation, the difference in the surface latent heat flux gets smaller in the absolute and relative sense. The surface latent heat flux is approximately 12 W m^{-2} (91%) higher in the first four days and only ≈2.5 W m^{-2} (4%) higher averaged over days 26 to 30, based on the small domain simulation set. Although u_* does remain higher for the forced simulations (figure 4), the near-surface gradient of moisture and temperature is reduced due to consistently increased exchange of heat and moisture with the sea surface. This negative feed-back on the fluxes in forced simulations is responsible for, what appear to be, slowly converging values of heat fluxes at later stages in forced and reference simulations.

As `ldr_forced` is initialized at t=14 days with the prognostic fields of `ldr_reference`, there is a still a larger near-surface moisture gradient. It appears

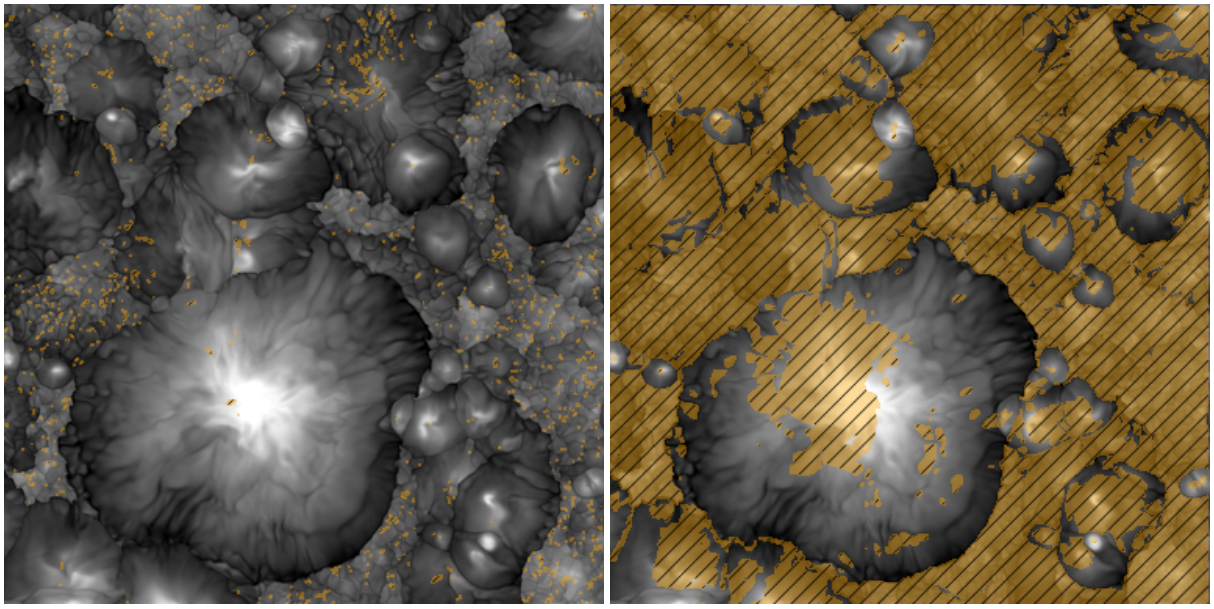

(a) $U_1 < 0.1$ m s^{-1} (1.3% of the domain) **(b)** $U_1 < 1$ m s^{-1} (61.9% of the domain)

Figure 5 – Horizontal cross sections of θ_e at z_1 for a 38.4 by 38.4 km subsection of `ldr_reference`. θ_e is coloured in grey scale linearly from white (339 K) to black (346 K). This cross section is taken at t=8.8 days. On top of the θ_e field is an orange hatched (semi transparent) mask which marks the grid points where U_1 is below either 0.1 or 1 m s^{-1} for sub plots **(a)** and **(b)** respectively.

this takes longer than a few days to adjust, given how the surface latent heat flux is still decreasing towards the end of the simulation as opposed to the other simulations, shown in figure 3. The difference in u_* between the large and small domain sets are similar, however.

4.2 Spatial differences

Figure 5 illustrates in what part of the domain wind values are typically below $\mathrm{U_{min}}$ for the two different values of $\mathrm{U_{min}}$ used in the simulations. The leading edge of cold pools, or the cold pool gust fronts, are the only source of strong winds in the simulation. In fact, from day one onwards, these cold pools are ever-present in all the simulations. Lowest θ_e values are found in the center of cold pool wakes, marked by the whitest areas in figure 5. Highest values are found at the cold pool gust front. It is along the edge of the gust fronts where the highest surface latent heat flux and moisture convergence are found, modifying the air to be more favourable for new convection to trigger. The cold pool wakes transform into regions of subdued convective activity instead of the increased convective activity near cold pool gust fronts or zones of convergence. Fluxes are increased is newly formed cold pool wakes compared to older ones, however, due to larger near-surface moisture gradients. It is in these cold pool wake regions that the minimum wind speed value is most often applied to. This is particularly well visible in sub-plot **(b)** of figure 5, illustrated by the orange hatched area marking grid points where $U_1 < \mathrm{U_{min}} = 1$ m s^{-1}. A significantly smaller, and arguably negligible, area of the example cross section has grid points where $U_1 < \mathrm{U_{min}} = 0.1$ m s^{-1}.

To make this result more quantitative, a probability density function (PDF) and cumulative density function (CDF) of U_1 is made (figure 6). The plot is based on four days of data, ending at day 20 to allow the large domains to be included in the comparison. Shorter time frames make the analyses sensitive to the chosen period, whereas taking a range of 4 days showed consistent results.

The most common wind speed is approximately 0.5 m s^{-1} and over 75% of the domain is covered with winds below 1 m s^{-1}. `ldr_forced` is clearly an outlier here, because it is still adjusting to a different RCE state, as was noted already in section 4.1.

Despite the similarities of the wind field and domain mean surface latent heat flux towards the end of the simulations, the spatial distribution of the surface latent heat flux is quite different. There is no sign of forced and reference simulations converging to the same spatial distribution of the surface latent heat flux, either. To illustrate this, box plots of the surface latent heat flux are made, shown in figure 7 for days 16 to 20 and in figure 9 for days 26 to 30. The former also contains `ldr_reference`. The figures illustrate the partitioning of latent heat input

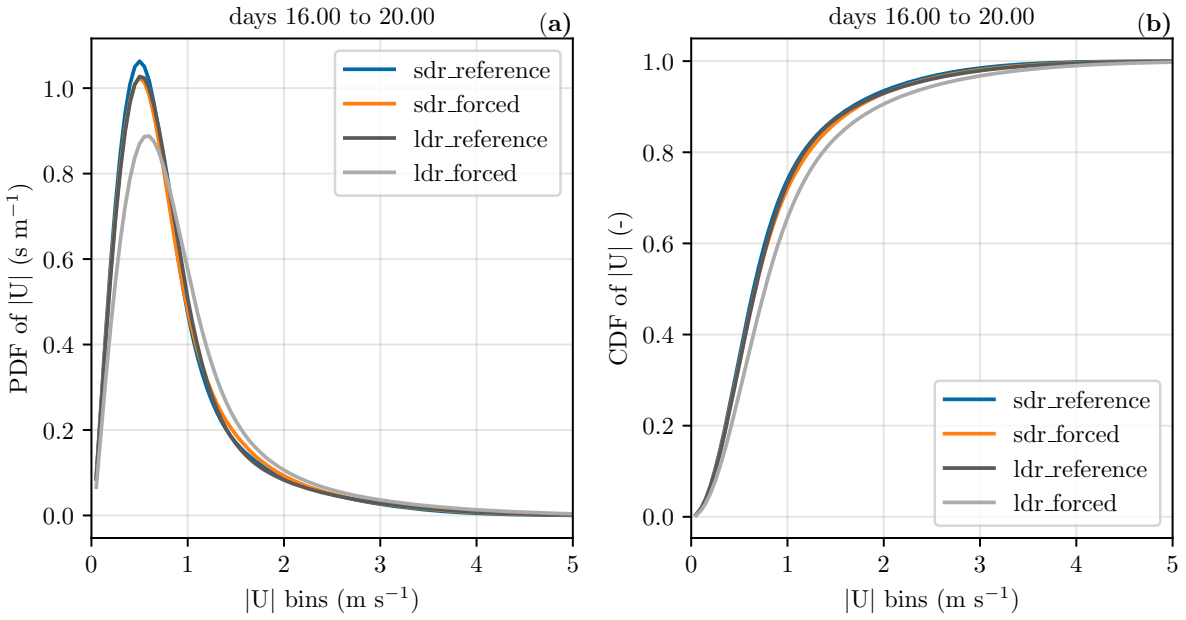

Figure 6 – Probability density function **(a)** and cumulative density function **(b)** of U_1 (at z=15 meters), based on horizontal cross sections from day 16 to 20 sampled every 360 seconds.

into the system in calm and convective regions. To be consistent with how $\mathrm{U_{min}}$ applies (in the case of forced simulations), calm and convective regions are separated into having U_1 below or above 1 m s^{-1}, respectively. An increase of 20% in the surface latent heat flux is seen in the forced simulation compared to the reference, a signal which rises above the temporal variance, given how the interquartile range of the boxes do not overlap. The box plots do overlap when the data is sampled in the convective regions, however. A decrease of 7% for the mean value is observed in the convective region. Domain size does not appear to have an impact on the mean, as the two reference simulations have nearly identical mean values. A smaller spread is seen in the large domain, however, likely because the values are trending in time and the large domain has 16 times as much spatial data to sample from. Even when the box plots are based on days 26 to 30, at which time the total flux between forced and reference simulations hardly differ, calm regions see an increase of 19% in the domain mean surface latent heat flux. 53% of the total surface flux comes from the calm region in the reference simulation. This value increases to 61% in the forced simulation (figure 9), meaning that the ratio between fluxes in calm and convective regions has increased by 39% (from 1.13:1 to 1.56:1 in calm versus convective) in favour of the calm regions.

4.3 Vertical profiles

Two clear indirect effects of a higher moisture input at the surface can be seen in figure 11 and 12. There is more total moisture in the lower part of the atmosphere, judging by the increased specific humidity q. The increase diminishes at 4 km and upwards. The troposphere warms up with an increased value of $\mathrm{U_{min}}$, an effect which, as opposed to q, becomes stronger with height.

4.4 Sensitivity

4.4.1 Domain size

A large domain allows for a greater spatial variance, which is indicated by higher values for the near-surface specific humidity q (figure 13). Despite the increased spatial variance, the temporal evolution and spatial distribution of the wind and latent heat exchange with the sea surface are very similar. Basing most of the analyses on the small domain set is therefore justified, as it also covers a complete and longer temporal range for both runs in the set.

4.4.2 Resolution and advection scheme

Only two different resolutions have been used, Δx = 100 m and 200 m. The results in terms of u_* and surface latent heat flux are similar, illustrated in figure 8. The forced version of the simulation with the `2i4` advection scheme is also consistent.

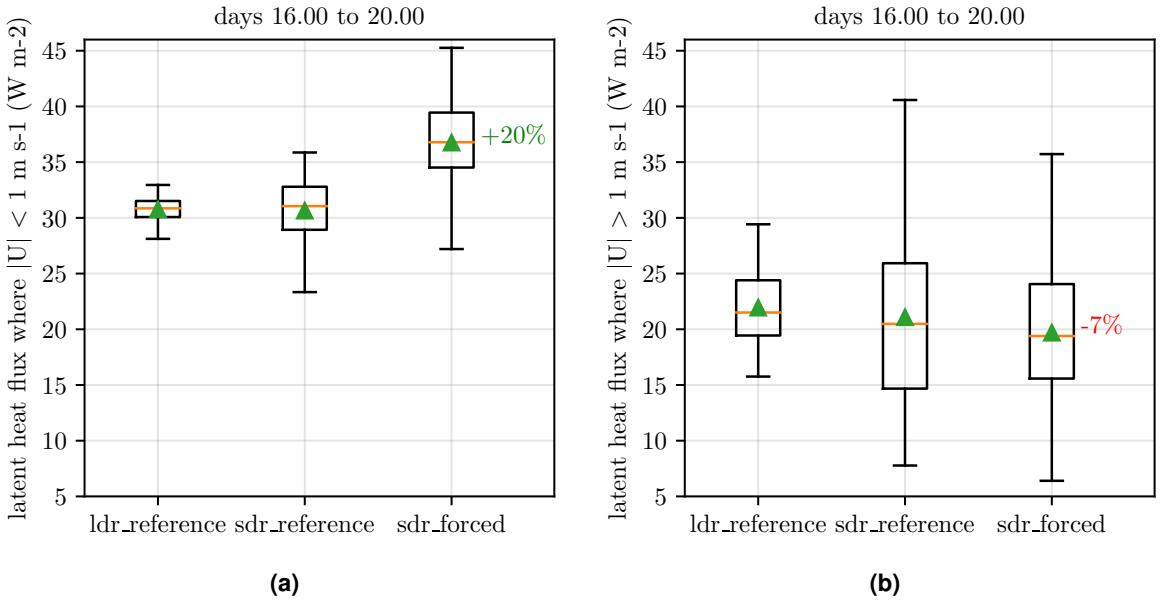

Figure 7 – Box plots of the surface latent heat flux from day 16 to 20, sampled every 360 seconds, where U_1 is below **(a)** or above **(b)** 1 m s^{-1}. The triangles represent the mean value, the center horizontal lines the median. The shown percentages refer to the difference between the mean flux values of `sdr_forced` and `sdr_reference`.

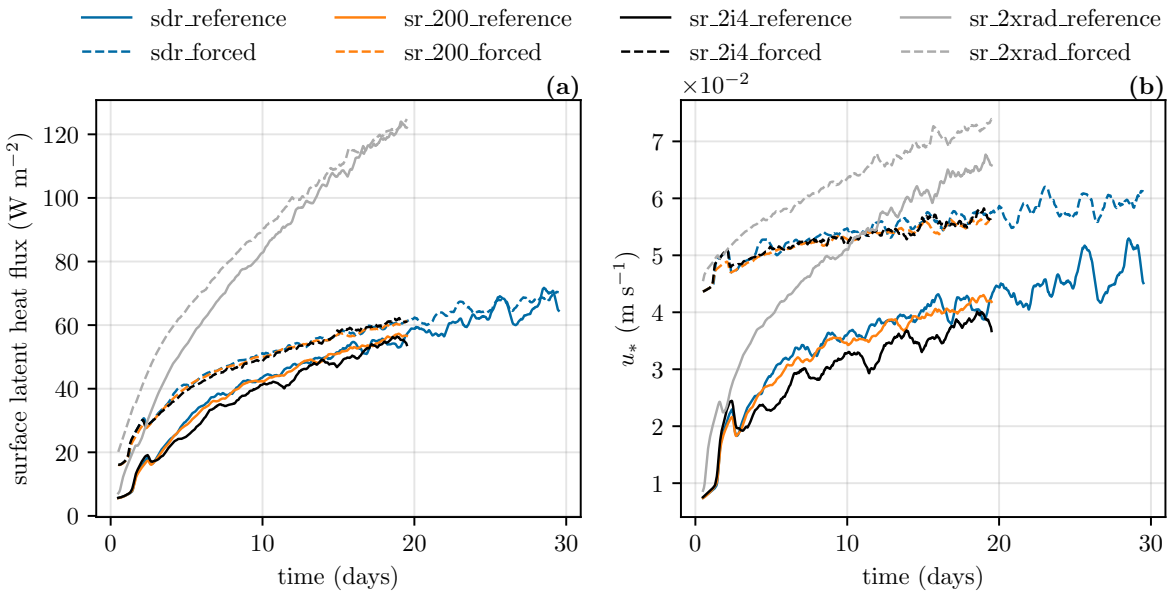

Figure 8 – Time series of all the small domain runs, spanning up to 30 days. A 24-hour centred moving average is applied to the time series data.

However, the reference version seems to be trailing behind and shows consistently lower values of both the surface latent heat flux and u_*. This only further increases the contrast between reference and forced simulations.

4.4.3 Cooling profile

When the prescribed radiative cooling is doubled, the difference between the reference and forced simulations becomes smaller. Wind speeds are ≈50% higher than in all other simulations run on the small domain. Surface fluxes are approximately twice as high when the cooling is doubled,

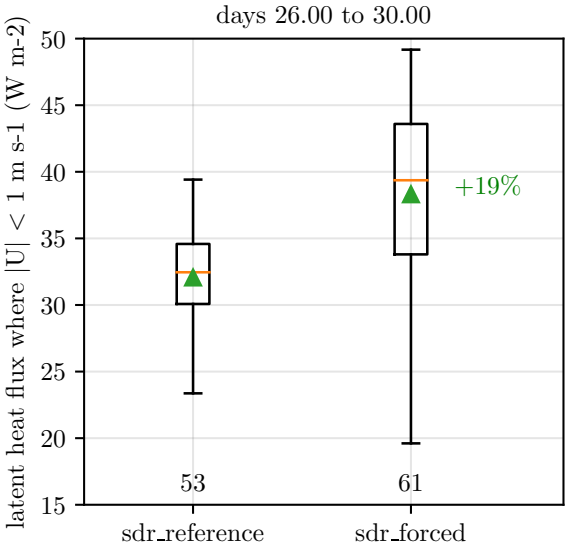

Figure 9 – Box plot similar to figure 7, but for days 26 to 30 of the small domain runs. The number below each box shows the percentage of total domain-mean flux.

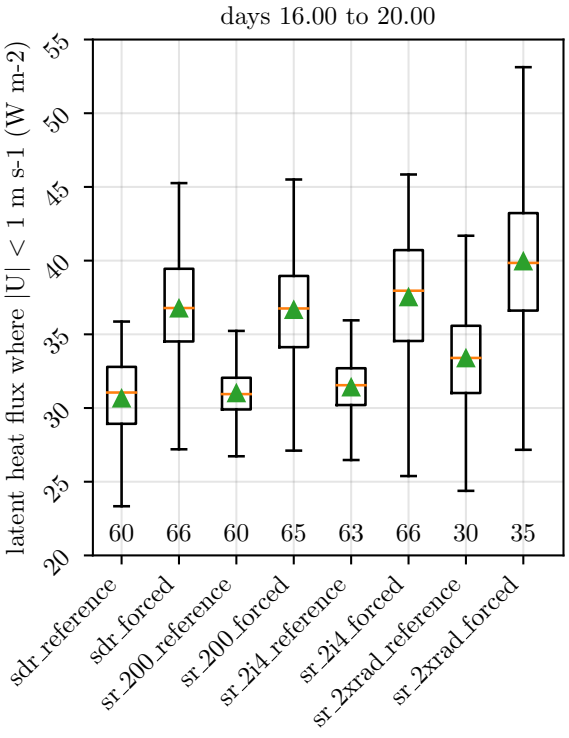

Figure 10 – Box plot for the sensitivity runs. Layout is similar to figure 9.

which is an expected response. Based on the box plots illustrated in figure 10, the change in partitioning between the calm and convective regions are still of the same magnitude. The fraction of surface latent heat flux in the calm region compared to the

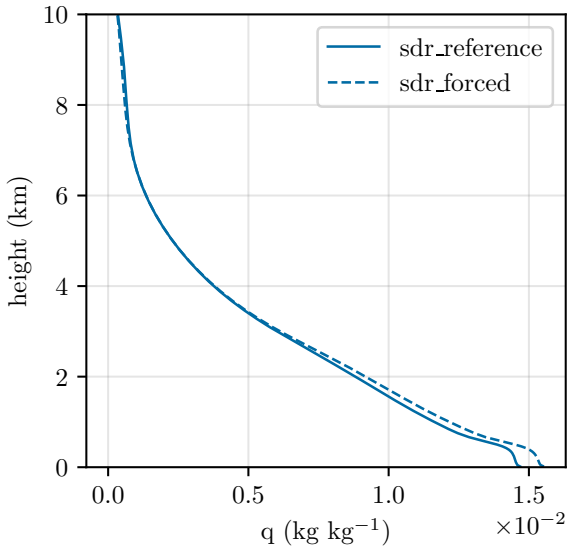

Figure 11 – Domain-mean vertical profile of the (total) specific humidity averaged over days 10 to 20.

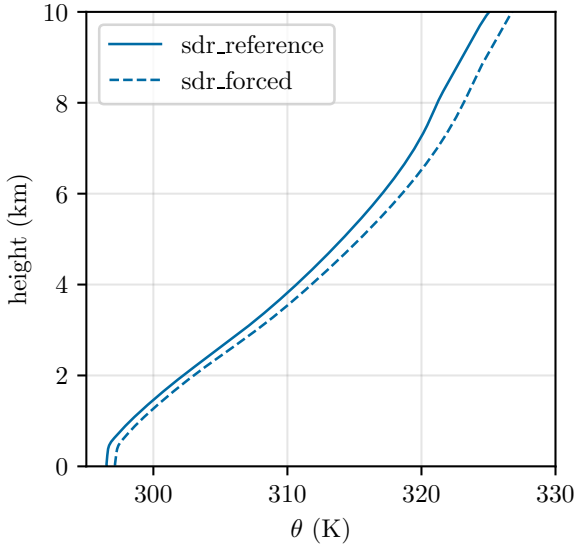

Figure 12 – Domain-mean vertical profile of θ averaged over days 10 to 20.

domain mean total is halved, however.

5 Discussion

Based on the results presented in section 4, the latent energy input into the atmosphere from the surface is sensitive to the chosen value of $\mathrm{U_{min}}$. Changes are observed in both the temporal and spatial sense, though the spatial differences are more interesting in relation to the surface flux feedback as a self-aggregation mechanism. The

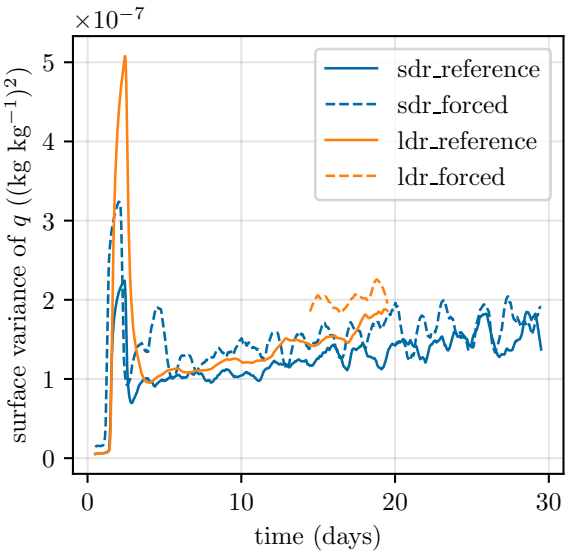

Figure 13 – Spatial variance of the (total) specific humidity at the lowest model level z_1. A 24-hour centred moving average is applied to the data.

modification of the near-surface moisture field is strongly influenced by cold pool dynamics (section 2.2), given how these cold pools in their early stages redistribute moisture and in their later stages form regions of little wind with a larger near-surface specific humidity gradient. The chosen value for $\mathrm{U_{min}}$ might influence the life-time of the subdued convective activity in cold pool wakes, as a higher value for $\mathrm{U_{min}}$ increases the surface moisture flux. The time it takes to average out most of the temporal variation in the PDFs of the wind field, approximately 4 days, suggests there is variability on a time scale longer than the cold pools, however. This averaging was mostly done to compare the results of the small domains, so it might be an indirect effect of the limited domain size.

While the domain size, even for the large domain runs, is not large enough to simulate self-aggregation, there is still evidence the surface flux feedback mechanism strength is reduced the higher the value of $\mathrm{U_{min}}$. An increase of approximately 20% in the surface latent heat flux is seen in reference versus forced simulations in the region where $U_1 < 1$ m s^{-1}. Since the surface flux feedback mechanism is currently seen as insufficient to on itself cause self-aggregation (in the rotation-free case), it is worth investigating whether this in fact holds true when the surface latent heat flux in the calm environment is further reduced. LES, despite its high computational demand in domains large enough for self-aggregation, seems more suited answer this question, as it does hardly has to deal with parametrizations to prevent L from becoming zero; U_1 is rarely below 0.1 m s^{-1}.

This would of course require an interactive radiation scheme, unlike what is done in this research. However, the contrast of surface latent heat flux between calm and convective regions changed approximately as much in the experiment where the prescribed radiative cooling is doubled. Therefore, the sensitivity to radiation might not overshadow the effect $\mathrm{U_{min}}$ has on the surface fluxes.

Indirect effects of an increase value of $\mathrm{U_{min}}$ are hard to find. Though the ABL becomes moister and the free troposphere warms through more latent heat release with a higher $\mathrm{U_{min}}$, the dynamics are similar. Only in the early stages do simulations with a higher $\mathrm{U_{min}}$ show more convective activity. What is interesting, though, is an increase in the spatial variance of the near-surface specific humidity field, despite how a higher $\mathrm{U_{min}}$ works to decrease the contrast between calm and convective regions. This would actually favour self-aggregation, which is characterized by an increasing contrast of moisture. It is hard to say whether the increased contrast with a higher $\mathrm{U_{min}}$ counteracts the potential decrease of the surface flux feedback strength without performing a sensitivity experiment better designed for this than what is done in this research.

6 Conclusion

We looked at the influence of the surface layer formulation to RCE simulations in the context of RCEMIP, a modelling project aiming to better understand the phenomenon of large scale convective self-aggregation. MOST-based parametrizations of the surface layer will fail in the free convection limit due to the Obukhov length L becoming zero. One way of preventing issues in this limit is by applying a minimum value $\mathrm{U_{min}}$ to the wind speed magnitude at the lowest model level in the parametrization scheme. By performing large-eddy simulations based on the 300 K RCEMIP case, we tested the sensitivity of the evolution of the RCE state and the surface flux feedback to different values of $\mathrm{U_{min}}$. Specifically, we test $\mathrm{U_{min}}$ = 1 m s^{-1}, as suggested for RCEMIP simulations compared to $\mathrm{U_{min}}$ = 0.1 m s^{-1}.

A higher value of $\mathrm{U_{min}}$ results in a different temporal evolution and spatial distribution of the surface latent heat flux. There is significantly more moisture in the ABL and the free troposphere is warmer. This is a result of the fact that for all simulation, at least 70 of the domain has a value for U_1 below 1 m s^{-1}. The surface latent heat flux in the calm regions, typically cold pool wakes, is increased by approximately 20%, reducing the potential strength of the surface flux feedback as a

self-aggregation mechanism. The domains sizes used for the simulations are too small to develop self-aggregation and thus do not show this feedback mechanism at work, as expected. The contrast of the near-surface specific humidity is increased in larger domains, however, and is further increased with a higher value for $\mathrm{U_{min}}$. The latter suggests there might also be changes to the dynamics in the simulation and this increased contrast could also be more favourable for self-aggregation to form. Results are consistent across a set of sensitivity tests, including a run with half the horizontal resolution. Therefore, to better test sensitivity of the surface flux feedback mechanism on $\mathrm{U_{min}}$, we suggest for further research to reduce the resolution and increase the domain size.

References

A. C. M. Beljaars. The parametrization of surface fluxes in large-scale models under free convection. *Quarterly Journal of the Royal Meteorological Society*, 121(522):255–270, jan 1995. doi: 10.1002/qj.49712152203. URL https://doi.org/10.1002/qj.49712152203.

ECMWF. *Part IV : Physical processes*, chapter 3.2. Number 4 in IFS Documentation. ECMWF, nov 2018.

C. C. van Heerwaarden, B. J. H. van Stratum, T. Heus, J. A. Gibbs, E. Fedorovich, and J. P. Mellado. MicroHH 1.0: a computational fluid dynamics code for direct numerical simulation and large-eddy simulation of atmospheric boundary layer flows. *Geoscientific Model Development*, 10(8):3145–3165, aug 2017. doi: 10.5194/gmd-10-3145-2017. URL https://doi.org/10.5194/gmd-10-3145-2017.

I. M. Held, R. S. Hemler, and V. Ramaswamy. Radiative-convective equilibrium with explicit two-dimensional moist convection. *Journal of the Atmospheric Sciences*, 50 (23):3909–3927, dec 1993. doi: 10.1175/1520-0469(1993)050⟨3909:rcewet⟩2.0.co;2. URL https://doi.org/10.1175/1520-0469(1993)050<3909:rcewet>2.0.co;2.

U. Högström. Non-dimensional wind and temperature profiles in the atmospheric surface layer: A re-evaluation. *Boundary-Layer Meteorology*, 42 (1-2):55–78, jan 1988. doi: 10.1007/bf00119875. URL https://doi.org/10.1007/bf00119875.

L. Schlemmer and C. Hohenegger. Modifications of the atmospheric moisture field as a result of cold-pool dynamics. *Quarterly Journal of the Royal Meteorological Society*, 142(694):30–42, sep 2015. doi: 10.1002/qj.2625. URL https://doi.org/10.1002/qj.2625.

A. Seifert and K. D. Beheng. A two-moment cloud microphysics parameterization for mixed-phase clouds. part 1: Model description. *Meteorology and Atmospheric Physics*, 92(1-2):45–66, oct 2005. doi: 10.1007/s00703-005-0112-4. URL https://doi.org/10.1007/s00703-005-0112-4.

L. J. Wicker and W. C. Skamarock. Time-splitting methods for elastic models using forward time schemes. *Monthly Weather Review*, 130(8):2088–2097, aug 2002. doi: 10.1175/1520-0493(2002)130⟨2088:tsmfem⟩2.0.co;2. URL https://doi.org/10.1175/1520-0493(2002)130<2088:tsmfem>2.0.co;2.

D. K. Wilson. An alternative function for the wind and temperature gradients in unstable surface layers. *Boundary-Layer Meteorology*, 99(1):151–158, apr 2001. doi: 10.1023/a:1018718707419. URL https://doi.org/10.1023/a:1018718707419.

A. A. Wing, K. Emanuel, C. E. Holloway, and C. Muller. Convective self-aggregation in numerical simulations: A review. *Surveys in Geophysics*, 38(6):1173–1197, feb 2017. doi: 10.1007/s10712-017-9408-4. URL https://doi.org/10.1007/s10712-017-9408-4.

A. A. Wing, K. A. Reed, M. Satoh, B. Stevens, S. Bony, and T. Ohno. Radiative–convective equilibrium model intercomparison project. *Geoscientific Model Development*, 11(2):793–813, mar 2018. doi: 10.5194/gmd-11-793-2018. URL https://doi.org/10.5194/gmd-11-793-2018.

J. C. Wyngaard. *Turbulence in the Atmosphere*. Cambridge University Press, 2010.

P. Zuidema, G. Torri, C. Muller, and A. Chandra. A survey of precipitation-induced atmospheric cold pools over oceans and their interactions with the larger-scale environment. *Surveys in Geophysics*, 38(6):1283–1305, nov 2017. doi: 10.1007/s10712-017-9447-x. URL https://doi.org/10.1007/s10712-017-9447-x.